International Journal of Astrobiology 12 (2): 149–160 (2013)
doi:10.1017/S1473550413000013

Synthesis of goethite in solutions of artificial seawater and amino acids: a prebiotic chemistry study

Cristine E. A. Carneiro[1], Flávio F. Ivashita[2], Ivan Granemann de Souza Junior[3], Cláudio M. D. de Souza[1], Andrea Paesano Jr[2], Antonio C. S. da Costa[3], Eduardo di Mauro[4], Henrique de Santana[1], Cássia T. B. V. Zaia[5] and Dimas A. M. Zaia[1]

[1]*Laboratório de Química Prebiótica, Departamento de Química-CCE, Universidade Estadual de Londrina, 86051-990 Londrina, PR, Brazil*
e-mail: damzaia@uel.br
[2]*Departamento de Física-CCE, Universidade Estadual de Maringá, 87020-900 Maringá, PR, Brazil*
[3]*Departamento de Agronomia-CCA, Universidade Estadual de Maringá, 87020-900 Maringá, PR, Brazil*
[4]*Laboratório de Fluorescência e Ressonância Paramagnética Eletrônica (LAFLURPE)-CCE, Universidade Estadual de Londrina, 86051-990 Londrina, PR, Brazil*
[5]*Departamento de Ciências Fisiológicas-CCB, Universidade Estadual de Londrina, 86051-990 Londrina, PR, Brazil*

Abstract: This study investigated the synthesis of goethite under conditions resembling those of the prebiotic Earth. The artificial seawater used contains all the major elements as well as amino acids (α-Ala, β-Ala, Gly, Cys, AIB) that could be found on the prebiotic Earth. The spectroscopic methods (FT-IR, EPR, Raman), scanning electron microscopy (SEM) and X-ray diffraction showed that in any condition Gly and Cys favoured the formation of goethite, artificial seawater plus β-Ala and distilled water plus AIB favoured the formation of hematite and for the other synthesis a mixture of goethite and hematite were obtained. Thus in general no protein amino acids (β-Ala, AIB) favoured the formation of hematite. As shown by surface enhanced Raman spectroscopy (SERS) spectra the interaction between Cys and Fe^{3+} of goethite is very complex, involving decomposition of Cys producing sulphur, as well as interaction of carboxylic group with Fe^{3+}. SERS spectra also showed that amino/CN and C-CH_3 groups of α-Ala are interacting with Fe^{3+} of goethite. For the other samples the shifting of several bands was observed. However, it was not possible to say which amino acid groups are interacting with Fe^{3+}. The pH at point of zero charge of goethites increased with artificial seawater and decreased with amino acids. SEM images showed when only goethite was synthesized the images of the samples were acicular and when only hematite was synthesized the images of the samples were spherical. SEM images for the synthesis of goethite with Cys were spherical crystal aggregates with radiating acicular crystals. The highest resonance line intensities were obtained for the samples where only hematite was obtained. Electron paramagnetic resonance (EPR) and Mössbauer spectra showed for the synthesis of goethite with artificial seawater an isomorphic substitution of iron by seawater cations. Mössbauer spectra also showed that for the synthesis goethite in distilled water plus Gly only goethite was synthesized and in artificial seawater plus Cys a doublet due to interaction of iron with artificial seawater/Cys was observed. It should be pointed out that EPR spectroscopy did not show the interaction of iron with artificial seawater/Cys.

Received 25 September 2012, accepted 4 January 2013, first published online 7 February 2013

Key words: amino acids, goethite, hematite, prebiotic chemistry, seawater.

Introduction

The reactions and the chemical complexes formed by iron are very important in several fields of science and technology such as metallurgy, pure chemistry, medicine, industrial chemistry, soil science and environmental science (Webb *et al*. 1999; Cornell & Schwertmann 2003). It also should be noted that iron is the fourth most abundant element in the crust of Earth. Iron oxide–hydroxides are widespread in nature and can be found in soils, rocks, lakes, rivers, sea floor and living organisms (Wade *et al*. 1999; Bishop & Murad 2002; Cornell & Schwertmann 2003) as well as in meteorites, on the surface of Mars and in interplanetary dust particles (IDPs) (Rietmeijer 1996; Catling & Moore 2003; Faivre & Zuddas 2006). For all iron oxide–hydroxides the basic structural unit is octahedron, where each Fe atom is surrounded by six O or OH ions (Cornell & Schwertmann 2003).

Since the early periods of the formation of the Earth, minerals and organic matter always coexisted; thus the interaction between them is an important issue for the prebiotic chemistry (Cleaves *et al*. 2012; Zaia 2012). In the oldest rock with over 3.70 billion years, banded iron formation, mainly in the form of hematite, was found (Moorbath 1977). Braterman *et al*. (1983) showed that Fe^{2+} could be oxidized to Fe^{3+} by UV

radiation. Under hydrothermal conditions, Fe^{2+} in the rocks (olivine) reduces H_2O to produce Fe^{3+}, H_2 and hydrocarbons (Martin *et al.* 2008). There were two sources of amino acids on the prebiotic Earth: exogenous amino acids synthesized outside the Earth, and endogenous amino acids synthesized on Earth. The exogenous sources (meteorites, comets, IDPs) and endogenous sources (submarine hydrothermal vents, heated substances in solid state by lava from volcanoes or impact bolides or radiation and mixture of gases) could deliver a large amount and variety of amino acids to the prebiotic Earth. According to a review published by Zaia *et al.* (2008), the amino acids from endogenous sources are more similar to the composition of amino acids of the living beings and the amino acids from exogenous sources comprise relatively more non-protein amino acids. Thus amino acids and iron oxide–hydroxides are substances that could be easily found on the prebiotic Earth. The interaction between amino acids and iron oxide–hydroxides is an important issue for prebiotic chemistry and could thus provide a better understanding of how the life arose on Earth.

Several experiments have investigated the synthesis of iron oxide–hydroxides with amino acids/peptides such as: goethite/Cys (Cornell *et al.* 1990), hematite/L-Phe, L-Ser, L-Ala, L-Gln or L-Glu (Kandori *et al.* 2006), ferrihydrite–lepdocrocite/L-His, L-Thr or Cys (Mantion *et al.* 2008), magnetite/L-Lys (Durmus *et al.* 2009), hematite/L-Lys or D-Asn (Wang *et al.* 2009), magnetite/L-carnosine (Durmus *et al.* 2011), hematite/L-Glu or L-Asp or L-Lys or D-Asn (Wang *et al.* 2011). The main goal these experiments were not to investigate prebiotic chemistry, but to synthesize novel catalysts or for use in medical applications. As shown by Mantion *et al.* (2008), single amino acids can be a valuable tool for material chemists to fabricate and stabilize iron oxide crystal phases. Cornell *et al.* (1990) observed that Cys favoured the formation of goethite. According to Durmus *et al.* (2009), insulating magnetite with Lys increased activation energy. Kandori *et al.* (2006) and Wang *et al.* (2009, 2011) observed that amino acids have an effect on the shape and size of particles of hematite. Kandori *et al.* (2006) obtained spherical hematite particles using L-Phe, L-Ser, L-Ala and ellipsoidal hematite particles using L-Gln and L-Glu. Wang *et al.* (2009, 2011) experiments showed that acidic amino acids complexed with nanoparticles of α-Fe_2O_3 to form a spindle shape, whereas complexation with basic amino acids formed rhombohedrons. They also observed that an increase of the amount of amino acids generally resulted in a decrease in the size of the particles. The magnetite synthesized by Durmus *et al.* (2011) could be used for cell separation, diagnosis and targeted drug delivery for cancer therapy.

Iron oxide–hydroxides were also used in several experiments of prebiotic chemistry: adsorption of amino acids on akaganéite and wüstite (Holm *et al.* 1983), binding/interaction of nucleotides and polynucleotides with goethite and akaganéite (Holm *et al.* 1993), adsorption of adenine on magnetite (Cohn *et al.* 2001), adsorption amino acids on goethite (Norén *et al.* 2008), adsorption of cysteine on hematite, magnetite and ferrihydrite (Vieira *et al.* 2011) and oligomerization of glycine and alanine on goethite, hematite and akaganéite (Shanker *et al.* 2012).

In the present work, goethite was synthesized in distilled water, artificial seawater, distilled water plus amino acids and artificial seawater plus amino acids. Solutions always contained [0.15 mol l^{-1} of $Fe(NO_3)_3$ and 0.15 mol l^{-1} of amino acids], and the initial pH of the solution was 13.80. This initial pH was very basic, but as reviewed by Holm & Andersson (2005) and Holm *et al.* (2006), this range of pH and the temperature used in the experiments could have been found in hydrothermal environments. As reviewed by Zaia *et al.* (2008), the amino acids (α-Ala, β-Ala, Gly, Cys, AIB) used in this work could be found on the prebiotic Earth. The experimental conditions used in this paper are consistent with those of the prebiotic Earth. The synthesized samples of goethite were characterized using FTIR spectroscopy, Raman spectroscopy, Mössbauer spectroscopy, and Electron paramagnetic resonance (EPR spectroscopy), scanning electron microscopy (SEM) and X-ray diffraction to further investigate the interaction of amino acids with iron oxides.

Materials and methods

All the reagents were of the analytical grade P.A.

Materials

Amino acids

All amino acids were purchased from Sigma and used as received. Amino acid abbreviations are given according to the recommendations of the IUPAC-IUB commission on biochemical nomenclature: α-Alanine (α-Ala), β-Alanine (β-Ala), Glycine (Gly), Cysteine (Cys) and 2-aminoisobutiric acid (AIB).

Synthetic seawater

Artificial seawater was made by dissolving following salts in 1.0 litre of distilled water: 28.57 g sodium chloride, 3.88 g magnesium chloride, 1.787 g magnesium sulphate, 1.308 g calcium sulphate, 0.832 g potassium sulphate, 0.103 g potassium bromide and 0.0282 g boric acid.

Silver colloid

All glassware was washed with nitric acid (HNO_3/H_2O, 1 : 1-v/v). Silver nitrate ($AgNO_3$), sodium borohydride ($NaBH_4$), each of analytical reagent grade, were used to prepare the Ag colloidal solution. The solution of colloidal silver was prepared in deionized water after Xiaojuan *et al.* (2010). First, 8.5 mg $AgNO_3$ was dissolved in 50 ml deionized water and added dropwise to a 150 ml (1.0 mM) solution of $NaBH_4$, while stirring vigorously in an ice bath. After the complete addition of $AgNO_3$, the resulting pale-yellow solution was stirred and maintained at 10 °C for approximately 30 minutes. The extinction spectrum of silver colloidal prepared in this manner has an absorbance maximum at 415 nm.

https://doi.org/10.1017/S1473550413000013 Published online by Cambridge University Press

Synthesis of goethite

A volume of 400 ml of 2.5 mol l^{-1} of KOH was mixed slowly with 1650 ml of prefiltered 0.150 mol l^{-1} $Fe(NO_3)_3$ solution in a plastic box (20 cm × 13 cm × 10 cm) and the mixture was stirred vigorously. Goethite was also synthesized in the presence individual amino acids (α-Ala, β-Ala, Gly, Cys or AIB), which were added 0.248 mol, also in the presence of seawater ions using the recipe described in section 2.1.2 and in the presence of seawater plus individual amino acids. The box was closed with a lid and the dispersions were aged for 60 hour at 70 °C. Precipitate were then collected by centrifugation and redispersed in distilled water; this procedure was repeated five times. The precipitate harvested from each synthesis procedure was then lyophilized.

The synthesized materials were analysed using FTIR spectroscopy, Raman spectroscopy, EPR spectroscopy, Mössbauer spectroscopy, SEM and X-ray diffraction.

Methods

Determination of pH at point of zero charge (pH_{pzc})

The 100 mg goethite was weighted and to it was added 250 µl of distilled water or 1.0 mol l^{-1} KCl. The samples were stirred for 30 minutes and after 24 hour the pH was measured. The pH_{pzc} was calculated using the equation: $pH_{pzc} = 2\,pH$ (1.0 mol l^{-1} KCl) − pH (distilled water) (Uehara 1979).

FTIR spectroscopy

The IR spectra were recorded with a Shimadzu FTIR 8300 spectrophotometer from 400 to 4000 cm^{-1}, using pressed KBr disks with a resolution of 4 cm^{-1}, after 95 scans. FTIR spectra were analysed using the Origin program (8.0, 2007).

Raman spectroscopy

Raman spectra were obtained from solid samples with a micro-Raman spectrograph Renishaw in Via with a 633 nm laser line and 4 cm^{-1} resolution (Table 1).

Surface-enhanced Raman spectroscopy (SERS) spectra were obtained using a Raman Spectrometer DeltaNu with a 532 nm laser and a spectral resolution of 8 cm^{-1} (Fig. 1). DeltaNús software, using baseline features, was used to remove background fluorescence. Borohydride colloid was used to obtain the SERS effect.

EPR spectroscopy

The samples were submitted to EPR spectroscopy at X-band (ca. 9 GHz) with 20 G modulation amplitude and magnetic field modulation 100 kHz using a JEOL (JES-PE-3X) spectrometer at room temperature. DPPH (2,2-difenil-1-picril-hidrazil) was used as g-marker and the standard of line intensity, using its spectral line ($g \approx 2.0036$).

X-ray diffraction

Powder materials from the synthesis experiments were analysed by powder X-ray diffraction using a Shimadzu D 6000 diffractometer, CoKα radiation (40 kV, 30 mA), nickel filter in a step-scanning mode (0.02°2θ/0.6 second) and 5 to 65°2θ amplitude. All peaks positions were analysed using Grams 8.0 software.

Table 1. *Identification of the minerals after the synthesis using Raman and FTIR spectroscopy*

Synthesis variation	Goethite	Hematite
Distilled water	X/Y	
Seawater	X/Y	
Glycine	X/Y	
Glycine + seawater	X/Y	
α-Alanine	X/Y	X/Y
α-Alanine + seawater	X/Y	Y
β-Alanine	X/Y	X/Y
β-Alanine + seawater		X/Y
2-Aminoisobutíric acid		X/Y
2-Aminoisobutíric acid + seawater	X/Y	X/Y
Cysteine	X/Y	
Cysteine + seawater	X/Y	

X-Raman spectroscopy and Y-FTIR spectroscopy. The following bands of Raman spectra are characteristics of goethite-205, 247, 300, 386, 418, 481 and 549 cm^{-1} and hematite-226, 245, 292, 411, 497 and 612 cm^{-1}. The following bands of FTIR spectra are characteristics of goethite-460, 640, 795 and 890 cm^{-1}; hematite-453, 531, 591 and 770 (Cornell & Schwertmann 2003).

SEM

SEM images were collected using the Philips model produced by Quanta 200 (FEI), in scanning electron microscope and Microanalysis laboratory facilities at UEL, equipped with an energy dispersive X-ray (EDX) model INCA 200 at 30 keV. The samples were fixed on 'stubs' using carbon adhesive tape, and then coated with a layer of gold.

Mössbauer spectroscopy

Mössbauer spectroscopy characterizations were performed in transmission geometry, using a conventional Mössbauer spectrometer in constant acceleration mode, at room temperature. The γ-rays were provided by a $^{57}Co(Rh)$ source, with initial nominal activity of 50 mCi. The Mössbauer spectra were analysed with a non-linear least-squares routine, with Lorentzian line shapes. All isomer shift (IS) data given are relative to α-Fe.

Results and discussion

pH and pH_{pzc} of goethite synthesis experiments

Table 2 shows the pH of the solution after the synthesis and pH_{pzc}. The pH_{pzc} for pure goethite was 8.56 and goethite synthesized in seawater was 9.20; these values are consistent with values reported in the literature (Cornell & Schwertmann 2003; Kosmulski *et al.* 2003). As reviewed by Kosmulski *et al.* (2003) the average pH_{pzc} for pure goethite was 8.32 ± 0.89 (± standard deviation). For other mixtures of FeOOH, the average of pH_{pzc} was 7.25 ± 0.77. All iron oxide–hydroxides shown in Table 2, with two exceptions, are in the range of pH_{pzc} described by Kosmulski *et al.* (2003). In general, when the synthesis of goethite was performed with artificial seawater

https://doi.org/10.1017/S1473550413000013 Published online by Cambridge University Press

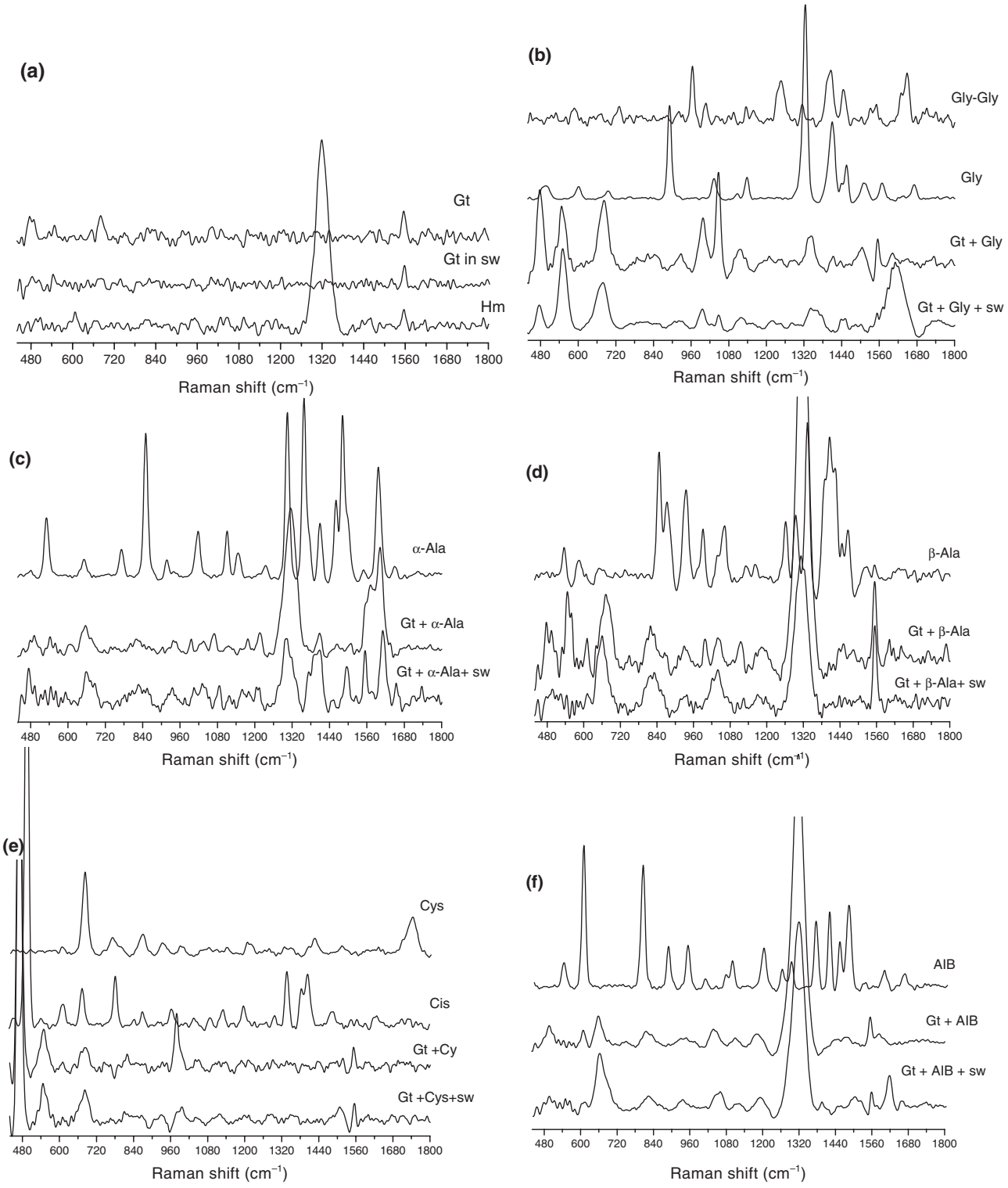

Fig. 1. EPR spectra of the goethite synthesized with and without seawater and amino acids. (), intensity of resonance Fe^{3+} $g \approx 2$ line; Gt, goethite; Hm, hematite; sw, artificial seawater; Gly, glycine; α-Ala, alanine; β-Ala, β-alanine; Cys, cysteine; AIB, 2-aminoisobutiric acid.

or artificial seawater plus amino acids an increase of pH_{pzc} was observed (by 0.66–1.94 pH units, Table 2). This increase was probably due to adsorption of seawater cations onto the surface of the goethite. Mohapatra *et al.* (2009) also observed an increase of pH_{pzc} when Mg^{2+} was included during the synthesis of goethite. Contrary to the effects of seawater, the pH_{pzc} of goethite synthesized in the presence amino acids was lower than that of pure goethite (Table 2). The interaction of the amino acids with Fe^{3+} of the goethite probably decreased the positive charge of the mineral, thus decreasing pH_{pzc}. A decrease of pH_{pzc} was also observed when goethite was synthesized in distilled water plus Cys and in artificial seawater

https://doi.org/10.1017/S1473550413000013 Published online by Cambridge University Press

Table 2. *pH of solutions after the synthesis of goethite under different conditions and pH at point zero charge (pH_{pzc})*

Synthesis variation[a]	pH	pH_{pzc}[b]
Pure	12.50	8.56
Seawater	12.20	9.20
Glycine	11.10	9.21
Glycine + seawater	11.05	9.15
α-Alanine	10.97	8.06
α-Alanine + seawater	12.45	9.16
β-Alanine	10.54	7.51
β-Alanine + seawater	10.25	9.45
2-Aminoisobutíric acid	8.77	8.34
2-Aminoisobutíric acid + seawater	12.11	9.60
Cysteine	11.53	5.07
Cysteine + seawater	11.47	3.59

[a] The condition of the synthesis was described in the methodology.
[b] The pH_{pzc} was determined as described by Uehara (1979).

plus Cys (Table 2). Thus the surface could be more positively or negatively charged depend on the medium (ions, molecules, etc) of the synthesis and it has an effect on pH_{pzc}. Cornell *et al.* (1990) observed that Cys promotes the rapid formation of goethite from ferric hydroxide, probably due to the interaction of sulphydryl group of Cys with Fe^{3+}.

In general, the salts of the seawater increased pH_{pzc} of goethite, whereas amino acids decreased. These effects are important for prebiotic chemistry since most of the molecules (amino acids, nucleic acid bases, etc) used in these experiments are charged. Thus the net charge of the goethite may mean difference between the adsorption (protection) and not adsorption (decomposition) of these molecules. If the molecules are not adsorbed onto minerals (protection), they could be decomposed by UV radiation or hydrolysis (Biondi *et al.* 2007).

FTIR and Raman spectroscopy of goethite synthesis experiments

Table 1 shows the identification of the minerals by FTIR and Raman spectroscopy after the synthesis of goethite with and without artificial seawater and amino acids. For the synthesis of goethite using distilled water, artificial seawater, distilled water plus Gly or Cys and artificial seawater plus Gly or Cys, only goethite was formed (Table 1). On the other hand, the synthesis of goethite in distilled water plus AIB and artificial seawater plus β-Ala favoured the formation of only hematite (Table 1). For the other synthesis experiments, a mixture of goethite and hematite were obtained (Table 1). The initial pH of reaction was 13.80 (KOH 2.5 mol l^{-1}); after synthesis of goethite the pH ranged from 8.77 to 12.50 (Table 2). According to Cornell & Schwertmann (2003), when synthesis of goethite is performed at pH below 12.00, hematite could also be synthesized. However, Cudennec & Lecerf (2006) showed that both low pH (2–5) and high pH (10–14) conditions favour the formation of goethite, whereas hematite is favoured at neutral pH (values around 7). The formation of goethite or hematite in this study appeared to depend on the pH and amino acid type (Tables 2 and 1). These results are showing that formation of mineral depends not only on temperature, water and salts, but also organic molecules (amino acids) could have had an important role. The mechanisms of the synthesis of these minerals are complex involving several steps (Flynn Jr 1984; Varanda *et al.* 2002; Lu *et al.* 2011).

SERS of amino acids and goethite synthesis experiments

Infrared spectroscopy was not useful for the characterization of our samples because FTIR spectra showed characteristic bands of amino acids only when goethite was synthesized in the presence of Cys. In general, Raman spectra of the samples showed a few bands belonging to amino acids, but many of them were too weak to be used for characterization. Thus the SERS was used to further investigate the synthesis experiments that included amino acids, as it is a powerful and convenient analytical tool that greatly enhances the weak signals derived from normal Raman spectroscopy.

Figure 2 shows the SERS spectra of Cys solid and the goethites synthesized with distilled water plus Cys and artificial seawater plus Cys. The SERS spectrum of Cys (Fig. 2) showed the following bands: 680, 843, 866, 927, 973 (shoulder) and 987, 1056, 1207, 1401, 1490 and 1509 and 1657 cm^{-1}, which were attributed to C–S stretching, HCS bending, C–COO^- stretching, HCN and HCH bending, NCH bending, C_α–N stretching, CH_2 twisting, COO^- stretching, CH_2 bending and NH_2 bending (Fleming *et al.* 2009). The SERS spectra of the samples of goethite synthesized with distilled water plus Cys and artificial seawater plus Cys showed enhanced of the bands at 981–990 and 981–1001 cm^{-1}, respectively; these bands were attributed to NCH bending (Fig. 2). The band at 1506 cm^{-1}, due to CH_2 bending, was also enhanced for all synthesis experiments (Fig. 2). These results suggest that probably these groups of Cys may be free and available to interact with Ag colloids. The SERS spectrum of solid Cys showed bands at 866 and 1402 cm^{-1}, due to C–COO^- stretching and COO^- stretching, respectively. Fleming *et al.* (2009) attributed the band at 1402 cm^{-1} to the interaction between the carboxylate group and metallic nanoparticles. However, these bands almost vanished when goethite was synthesized with distilled water plus Cys and artificial seawater plus Cys (Fig. 2). The vanishing of these bands could be due to the interaction between the carboxylic groups of Cys with goethite. The spectrum of solid Cys showed a band at 2577 cm^{-1} due to S–H stretching. This band vanished for the goethite samples (data not shown). This result could be an indication of the formation of Cistine or the interaction of sulphydryl group of Cys with Fe^{3+} or the decomposition of Cys. However, the spectra of these samples did not show the band at 500 cm^{-1} arising from the S–S stretching of Cistine. The spectrum did exhibit a band at 470 cm^{-1} that matched with the spectrum of sulphur (data not shown). These data suggest that Cys was decomposed during the experiment. The results above indicate complex interactions between Cys, seawater ions and Fe^{3+} during the synthesis of goethite.

Figure 2 shows the SERS spectrum of α-Ala solid, goethites synthesized with distilled water plus α-Ala, and artificial seawater plus α-Ala. The SERS spectrum of α-Ala (Fig. 2)

https://doi.org/10.1017/S1473550413000013 Published online by Cambridge University Press

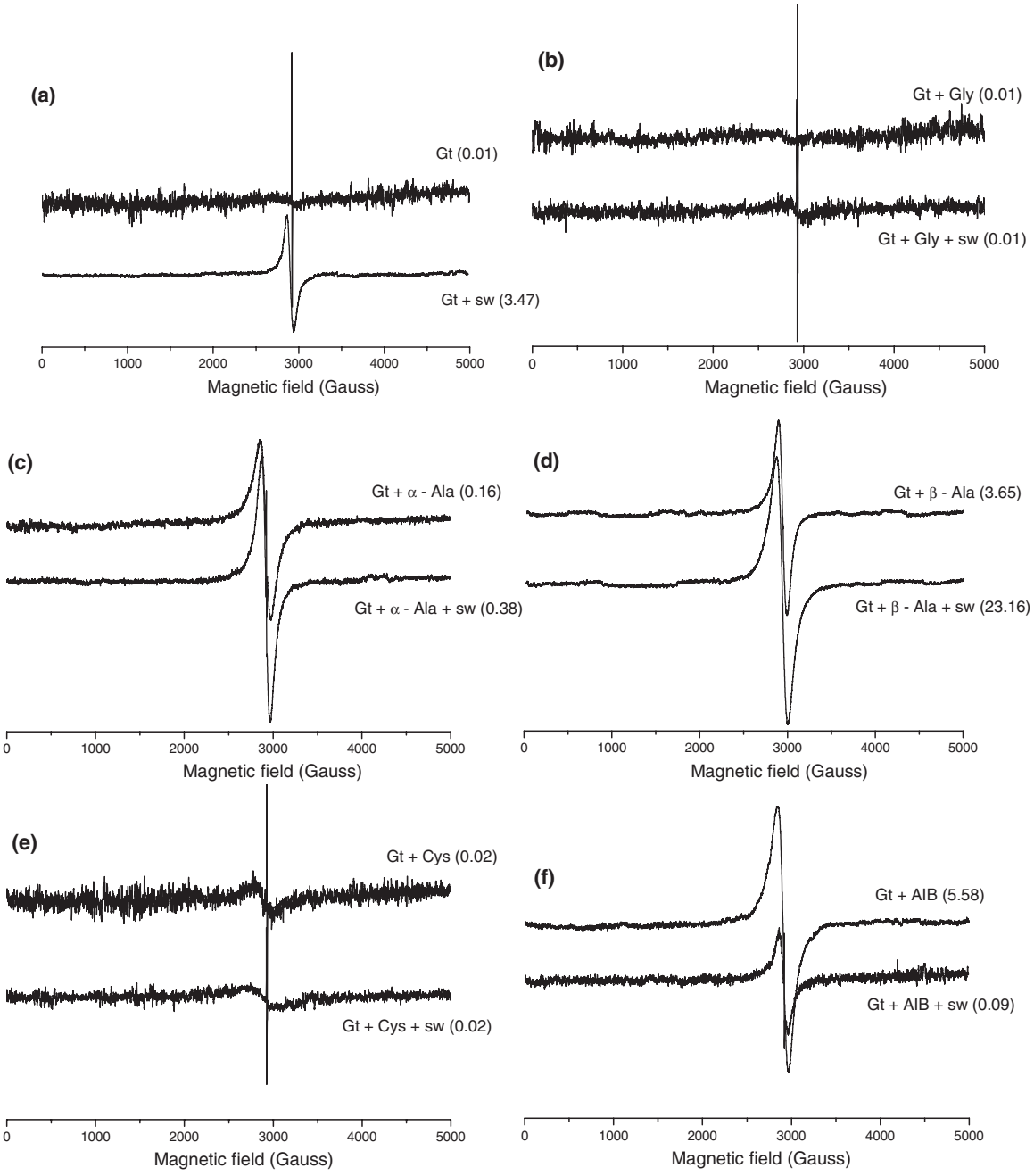

Fig. 2. Raman spectra of the goethite synthesized with and without seawater and amino acids. Gt, goethite; Hm, hematite; SW, artificial seawater; Gly, glycine; α-Ala, alanine; β-Ala, β-alanine; Cys, cysteine; AIB, 2-aminoisobutiric acid.

showed the following bands 850, 917, 1015, 1112, 1146, 1233, 1362, 1375, 1409, 1460, 1482–1549, 1596 and 1650 cm^{-1} attributed to C–CH_3 stretching, C–COO^- stretching, CH_3 rocking, CN stretching, NH_2 twisting, NH_3^+ rocking, CH_3 symmetric deformation, CH_3 asymmetric deformation, COO^- stretching, CH_3 rocking, CH rocking, NCC deformation and $C_\beta C_\alpha C$ deformation (Kapitán *et al*. 2006). The strong band in the region 850 cm^{-1} can be considered as a marker of α-Ala (Zhu *et al*. 2011); however, this band vanished in synthesized materials. The SERS spectrum of the sample of goethite synthesized with distilled water plus α-Ala showed the bands at 530–568, 609, 637–692, 1375, 1409, 1460, 1482, 1500, 1596 and 1650 cm^{-1}. For the sample of goethite synthesized with artificial seawater plus α-Ala, the following bands were observed 474–619, 650–686, 756–864, 1375, 1409, 1477, 1495, 1500, 1610 and 1650 cm^{-1}. Raman spectra showed that the bands of the samples are shifted but there are very few bands that could be attributed to α-Ala (1375, 1409, 1460, 1477–500, 1650 cm^{-1}); thus these bands were enhanced by SERS. The bands due to amino/CN (1112, 1146, 1233 cm^{-1}) and C–CH_3 (850 cm^{-1}) groups were not enhanced by SERS probably because these groups are interacting with iron atoms of goethite.

Figure 2 shows the shifting of several bands for the samples of goethite synthesized with amino acids (Gly, AIB, β-Ala) plus

https://doi.org/10.1017/S1473550413000013 Published online by Cambridge University Press

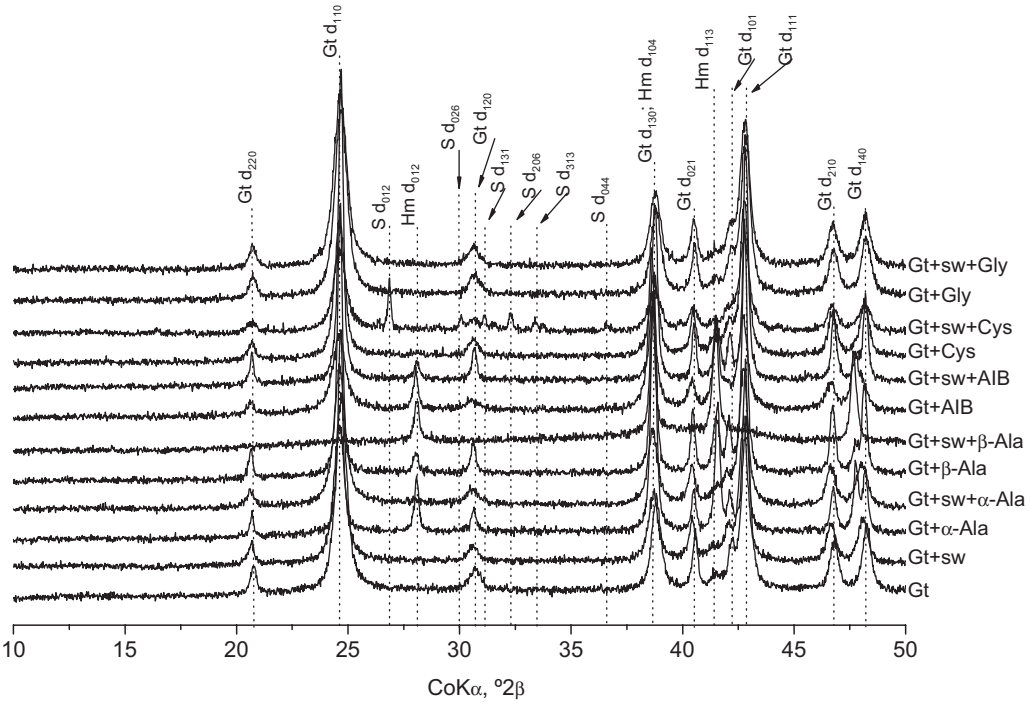

Fig. 3. X-ray diffraction patterns for the synthesized goethite with and without seawater and amino acids. Gt, goethite; Hm, hematite; sw, artificial seawater; Gly, glycine; α-Ala, alanine; β-Ala, β-alanine; Cys, cysteine; AIB, 2-aminoisobutiric acid.

distilled water and amino acids (Gly, AIB, β-Ala) plus artificial seawater. However, it was not possible to say which amino acid groups are interacting with Fe^{3+}.

EPR spectroscopy

Goethite synthesis in distilled water and seawater

Figure 1 shows EPR spectra of goethite synthesized with distilled water, artificial seawater, distilled water plus amino acids and artificial seawater plus amino acids. For goethite synthesized with distilled water, the EPR spectrum showed a small resonance line at $g \approx 2$ (intensity 0.01) (Fig. 1). This result is consistent with that obtained by Guskos *et al.* (2002), because at room temperature, goethite exhibits antiferromagnet characteristics. In the antiferromagnet state, the spins are oriented along the *b*-axis, with up and down spins in alternate chains of octahedral (Cornell & Schwertmann 2003). However, goethite synthesized in artificial seawater showed a more intense resonance line at $g \approx 2$ (intensity 3.47) (Fig. 1). For this experiment results from FTIR, Raman spectroscopy (Table 1), X-ray diffraction (Fig. 3) and SEM (Fig. 4) all suggest that only goethite was synthesized. This resonance line could be attributed to interactions between Fe^{3+} and neighbours (O^{2-}, OH^{-}, cations of artificial seawater –Ca^{2+}–Mg^{2+}) in the crystalline chain. The ions Ca^{2+} and Mg^{2+} from artificial seawater are able to replace iron in the crystalline chain. These ions could also be occluded in the structure of goethite causing distortion of octahedral structure of Fe^{3+} and transforming its paramagnetic or ferromagnetic characteristics. Thus the observed increased in intensity at $g \approx 2$ was probably due to the interactions between Fe^{3+} and Ca^{2+}/Mg^{2+}.

Besides all the results from FTIR, Raman spectroscopy, X-ray diffraction and SEM suggest that only goethite was synthesized. However, the EPR spectroscopy is showing those goethites synthesized with and without artificial seawater are not the same.

Goethite synthesis in amino acids solutions

The samples of goethite synthesized with distilled water plus Gly (intensity 0.01) or Cys (intensity 0.02) and artificial seawater plus Gly (intensity 0.01) or Cys (intensity 0.02) showed a small intensity resonance line (Fig. 1). Gly and Cys prevent the interaction between Fe^{3+} and Ca^{2+}/Mg^{2+}. Gly likely complexed with Ca^{2+}/Mg^{2+} and prevented the occlusion of these ions or replacement of Fe^{3+} in the crystalline chain, which could cause the ferromagnetic effect (Smith *et al.* 1985). In experiments including Cys the sulphur forming the inner-sphere surface complex with iron appeared to improve the complete precipitation of goethite, similar to the results of Cornell & Schwertmann (2003). FTIR, Raman spectroscopy (Table 1) and X-ray diffraction measurements (Fig. 3) did not indicate the formation of iron oxides other than goethite in these synthesis experiments.

For the synthesis of goethite with distilled water plus α-Ala and artificial seawater plus α-Ala, the EPR spectra showed an increase in the intensity of line $g \approx 2$, probably due to the formation of hematite or ferromagnetic goethite (Table 1, Fig. 4). It should be noted that the intensity resonance line was higher in the sample of artificial seawater plus α-Ala than distilled water plus α-Ala, probably due to the effect of Ca^{2+}/Mg^{2+} in the structure of goethite and hematite (Fig. 1).

https://doi.org/10.1017/S1473550413000013 Published online by Cambridge University Press

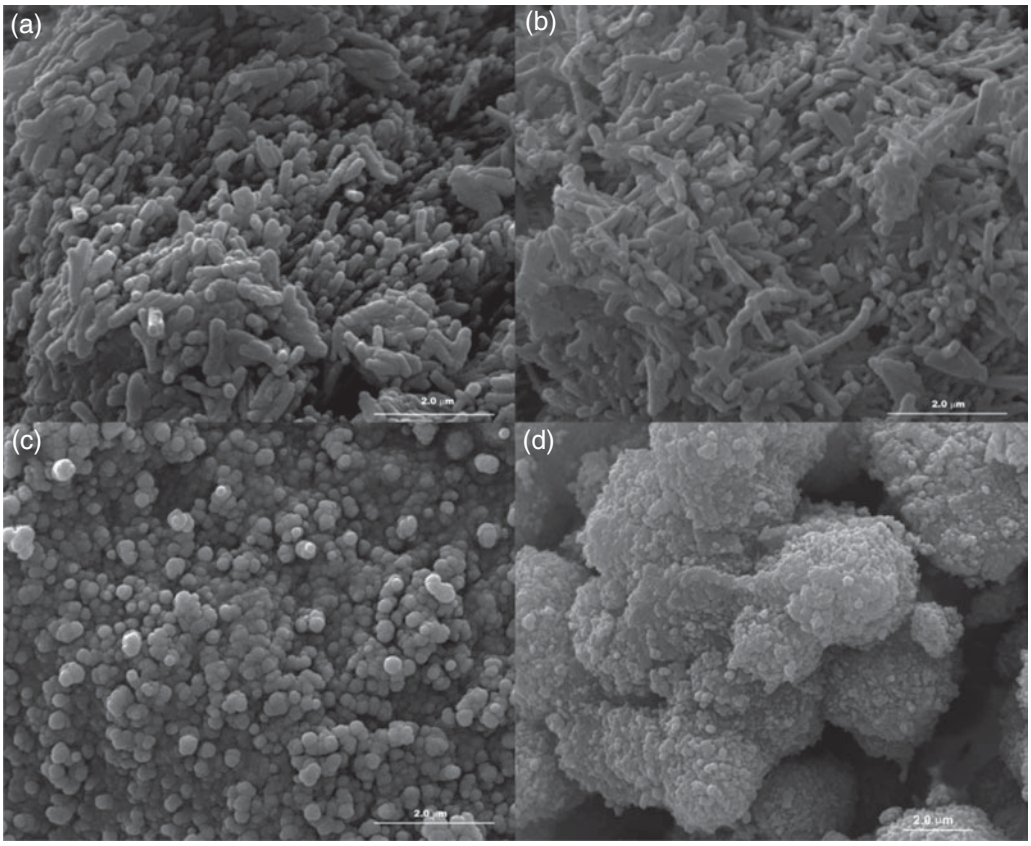

Fig. 4. SEM images of goethite. (a) goethite synthesized in distilled water, (b) goethite synthesized in artificial seawater, (c) goethite synthesized in distilled water plus AIB and (d) goethite synthesized in distilled water plus Cys.

The intensity resonance line for the synthesis of goethite with distilled water plus β-Ala was lower than the synthesis of goethite with artificial seawater plus β-Ala, because only hematite was synthesized in the latter experiment, as shown by FTIR and Raman spectroscopy (Table 1), and X-ray diffraction data (Fig. 3). The intensity of the resonance line for the samples of goethite synthesized with distilled water plus β-Ala was probably higher than the samples of distilled water plus α-Ala, because low crystalinity of the hematite in the samples of β-Ala (Fig. 3) and particles size (Zysler *et al.* 2003). However, it should be noted that the effect of size of particle on EPR signal is small when compared with the EPR signal due to the bulk of the sample (Zysler *et al.* 2003; Carbone *et al.* 2005).

The intensity of resonance lines of the sample of goethite synthesized with distilled water plus AIB was higher than the sample of artificial seawater plus AIB, because only hematite was synthesized in the former (Table 1, Figs 4 and 5). In general, as shown in (Table 1) the EPR results also indicate that synthesis experiments including protein amino acids favour the formation of goethite over hematite.

X-ray diffraction

Figure 3 shows X-ray diffractograms of goethite synthesized with distilled water, artificial seawater, distilled water plus amino acids and artificial seawater plus amino acids. As shown by FTIR and Raman spectroscopy (Table 1), X-ray diffractograms confirmed the synthesis of only goethite when the mineral was synthesized with distilled water, artificial seawater, distilled water plus Gly or Cys or artificial seawater plus Gly or Cys. In other synthesis experiments, X-ray diffractograms confirmed the synthesis of the hematite and goethite (Table 1, Fig. 3).

SEM

Figure 4 shows SEM images of goethite synthesized with distilled water, artificial seawater, distilled water plus AIB and distilled water plus Cys. For goethite synthesized in distilled water and artificial seawater, the images are expectedly acicular (Fig. 4) (Cornell & Schwertmann 2003; Villalobos *et al.* 2009). These results are in agreement with those of FTIR spectroscopy, Raman spectroscopy (Table 1), EPR spectroscopy (Fig. 1), Mössbauer spectroscopy (Table 3) and X-ray diffraction (Fig. 3). For the synthesis of goethite with distilled water plus AIB, hexagonal particles and spherical aggregates of hematite were formed (Fig. 4). Kandori *et al.* (2006) also observed spherical shape for hematite synthesized with several amino acids. For the synthesis of goethite with distilled water plus Cys (Fig. 4) and artificial seawater plus Cys (data not shown), we observed the formation of spherical crystal aggregates with radiating acicular crystals. The SEM images obtained for the samples of goethite synthesized with

https://doi.org/10.1017/S1473550413000013 Published online by Cambridge University Press

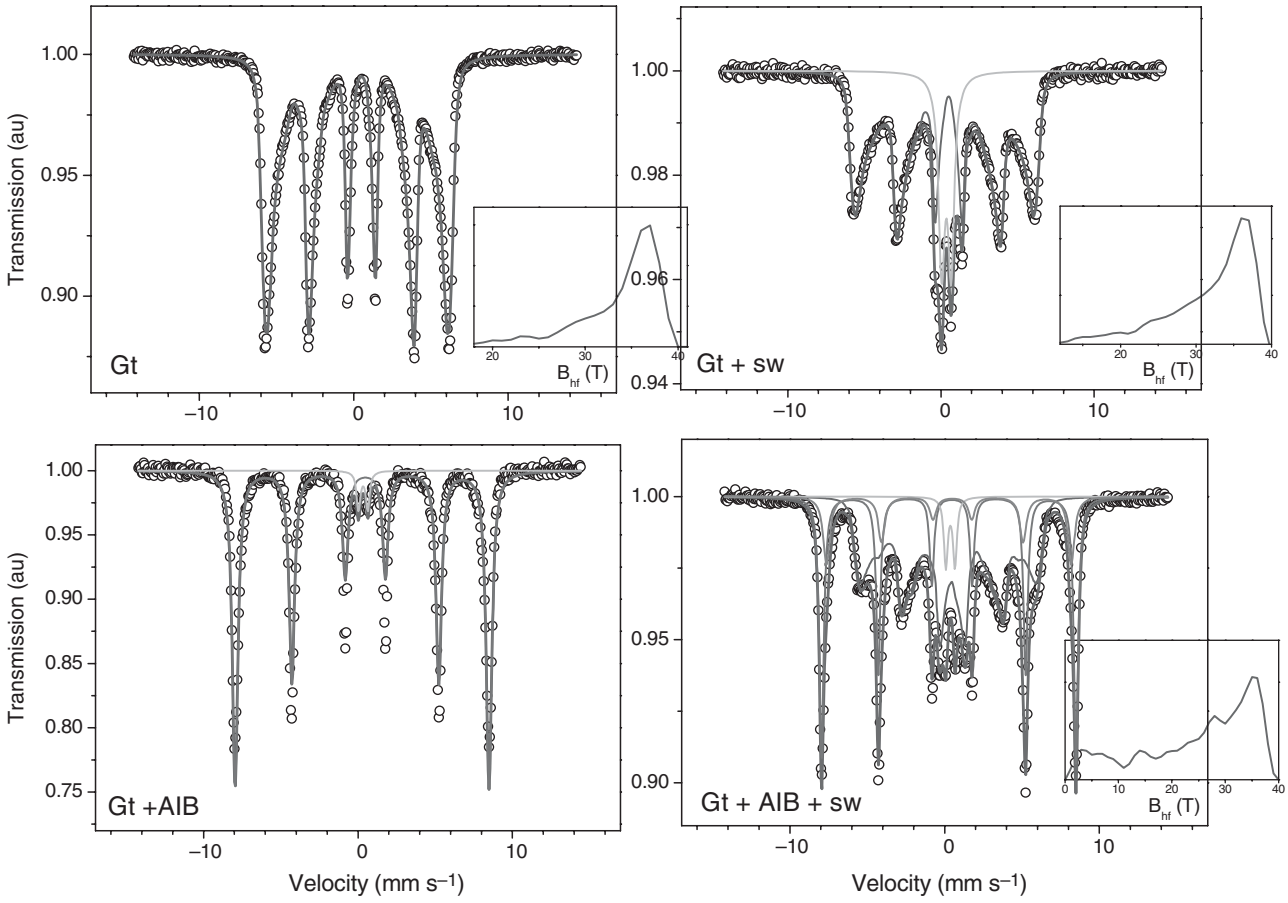

Fig. 5. Mössbauer spectra for the synthesized goethite with and without seawater and amino acids. Gt, goethite; sw, artificial seawater; AIB, 2-aminoisobutiric acid.

distilled water plus Gly and artificial seawater plus Gly were also acicular (data not shown). For the other goethite synthesis experiments, we observed a mixture of goethite (acicular) and hematite (spherical, hexagonal) (data not shown).

Mössbauer spectroscopy

Figure 5 shows some representative Mössbauer spectra obtained for goethite samples prepared under different conditions. All the spectra were fitted using a hyperfine magnetic field distribution, as usual for this iron hydroxide. Eventually, a doublet and a discrete sextet were included in the fit to account a paramagnetic fraction and highly oxidized iron magnetic states present in the samples, respectively. Table 3 lists the hyperfine parameters for all synthesized samples.

Goethite synthesis in distilled water and seawater

The B_{hf} of goethite in distilled water was 33.6, showing that only goethite was synthesized. Barrero *et al.* (2006) also using the $(FeNO_3)_3$ as precursor to goethite, observed a B_{hf} value of 37.0 T, showing that hyperfine magnetic properties strongly depend on synthesis conditions. This result is the same that was obtained using FTIR, Raman and EPR spectroscopy (Table 1, Fig. 1), X-ray diffraction (Fig. 3) and SEM images (Fig. 4). For goethite synthesized with artificial seawater, a decrease in B_{hf} was observed. A doublet whose area was about 20% of the total area was also observed, probably due to isomorphic substitution of iron by seawater cations (Table 3). The EPR spectrum of this sample also showed a change of the goethite when it was synthesized with artificial seawater (Fig. 3). An increase of the intensity line $g \approx 2$ was observed.

Goethite synthesis in amino acids solutions

For goethite synthesized with distilled water plus Gly and artificial seawater plus Gly, B_{hfs} were the same as goethite synthesized with distilled water, and the peak areas indicated that only goethite was synthesized. These results are the same that was obtained using FTIR, Raman and EPR spectroscopy (Table 1, Fig. 1) and X-ray diffraction (Fig. 3). Goethite synthesized with distilled water plus α-Ala or β-Ala showed the formation of goethite and hematite with areas 57.1/42.9 and 79.8/20.2%, respectively. The hematite showed a sextet about at 51 B_{hf}.

For goethite synthesized with artificial seawater plus α-Ala, in addition to the signals of goethite and hematite, a doublet was also observed, probably arising from the interaction of iron with cations of artificial seawater (Table 3). The results obtained with Mössbauer spectroscopy were consistent with other methods (Table 1, Figs 1 and 3). The sample of goethite synthesized with artificial seawater plus β-Ala showed the formation hematite with a value of B_{hf} 47.8 (Table 3).

https://doi.org/10.1017/S1473550413000013 Published online by Cambridge University Press

Table 3. *Mössbauer hyperfine parameters and subspectral areas for the synthesis of goethite with and without seawater and amino acids*

Synthesis	Subspectrum	Γ (mm/s)	δ (mm/s)	Δ (mm/s)	B_{hf} (T)	Area (%)
Distilled water	Dist	0.3	0.37	−0.26	33.6	100
Sw	Dist	0.3	0.37	−0.27	30.2	80.2
	Doublet	0.49	0.35	0.61	–	19.8
Gly	Dist	0.3	0.37	−0.27	33.6	100
Gly + sw	Dist	0.3	0.37	−0.26	32.7	100
α-Ala	Dist	0.3	0.37	−0.27	35.9	57.1
	Sextet	0.36	0.37	−0.2	51.1	42.9
α-Ala + sw	Dist	0.3	0.37	−0.26	30.8	83.2
	Doublet	0.77	0.38	0.65	–	12.1
	Sextet	0.36	0.35	−0.21	50.8	4.7
β-Ala	Dist	0.3	0.37	−0.26	36.1	79.8
	Sextet	0.36	0.37	−0.17	51.2	20.2
β-Ala + sw	Dist	0.3	0.38	−0.19	47.8	72.1
	Doublet	0.52	0.34	0.63	–	27.9
AIB	Doublet	0.3	0.33	0.59	–	4
	Sextet	0.43	0.37	−0.21	51	96
AIB + sw	Dist	0.3	0.37	−0.26	25	55.5
	Doublet	0.3	0.37	0.58	–	3.5
	Sextet	0.33	0.37	−0.21	51	29.4
	Sextet	0.51	0.38	−0.22	49	11.6
Cys	Dist	0.3	0.37	−0.27	32.4	91.6
	Doublet	1	0.37	0.47	–	8.4
Cys + sw	Dist	0.3	0.37	−0.26	30.9	90.8
	Doublet	0.36	0.37	0.57	–	9.2

Sw, artificial seawater; Gly, glycine; α-Ala, α-alanine; β-Ala, β-alanine; Cys, cysteine; AIB, 2-aminoisobutiric acid; Γ, half-width of spectral lines; δ, isomer shift (relative to α-iron); Δ, quadrupole splitting; B_{hf}, hyperfine magnetic field; Area, relative contribution of the component.

In general, the B_{hf} value for hematite was 51; however, lower values could be an indication of isomorphic substitution (Berquó *et al*. 2007).

For the sample of goethite synthesized with distilled water plus AIB, a sextet (B_{hf} 51) whose area of 96% was indicative of hematite and a doublet whose area was 4% was probably due to interaction of iron with AIB (Table 3). Hematite was also detected by other methods (Table 1, Figs 3 and 4). For the sample of goethite synthesized with artificial seawater plus AIB, a dist (B_{hf} 25) was observed likely due to the formation of goethite. Additionally, we observed two sextets (B_{hf} 49 and 51) due to hematite formation with different crystalline structures and a doublet probably due the interaction of iron with cations of artificial seawater (Table 3). FTIR, Raman (Table 1) and EPR (Fig. 1) spectroscopy and X-ray diffraction (Fig. 1) also indicated the synthesis of hematite and goethite.

For goethite synthesized with distilled water plus Cys and artificial seawater plus Cys, a dist (B_{hf} 32.4 and 30.9) was observed likely due to goethite formation. A doublet indicated the interaction of Cys with iron. For these synthesis experiments only goethite was detected by other methods (Table 1, Figs 1 and 3). However, the Mössbauer spectroscopy showing goethites synthesized with and without Cys are not the same.

Conclusion

The pH_{pzc} of goethites synthesized with artificial seawater increased, likely due to the adsorption of cations. Goethite synthesized with amino acids showed lower pH_{pzc} values, likely a result of the interaction of the amino acids with Fe^{3+} of the goethite, which would decrease the positive charge of the mineral.

The formation of goethite or hematite depended on the pH and the type of amino acid included during the synthesis experiments, in general, no protein amino acids favoured the formation of hematite.

FTIR and Raman spectroscopy showed that only goethite was synthesized in experiments with distilled water, artificial seawater, distilled water plus Gly or Cys and artificial seawater plus Gly or Cys. FTIR and Raman spectroscopy also showed that only hematite was synthesized in experiments with artificial seawater plus β-Ala and distilled water plus AIB. For the other synthesis experiments a mixture of goethite and hematite was obtained. All these results were confirmed by X-ray diffraction.

For the samples of goethite synthesized with distilled water plus Cys and artificial seawater plus Cys, SERS spectra showed that the interaction between Cys and Fe^{3+} of goethite is very complex involving decomposition and interaction of Cys groups with Fe^{3+}. For the experiments where goethite synthesized with distilled water plus α-Ala and artificial seawater plus α-Ala, the bands due to amino/CN and C–CH_3 groups were not enhanced during SERS effect, suggesting that these groups may be interacting with iron of goethite.

EPR spectroscopy confirmed the formation of only goethite in the synthesis with distilled water, distilled water

https://doi.org/10.1017/S1473550413000013 Published online by Cambridge University Press

plus Gly or Cys and artificial seawater plus Gly or Cys, as the antiferromagnet characteristic of goethite at room temperature exhibited weak resonance line intensity. However, an increase of the resonance line intensity was observed for the synthesis of goethite with artificial seawater, which probably resulted from interaction of iron with salts of the artificial seawater causing a distortion of octahedral iron. Thus Gly and Cys likely protected iron from the interaction with salts of artificial seawater. The highest resonance line intensities were obtained for the samples of goethite synthesized with distilled water plus AIB and artificial seawater plus β-Ala, because only hematite was obtained. For the other synthesis experiments a mixture of goethite and hematite was obtained then an increase of the resonance line intensity was also observed.

For experiments that appeared to result in the synthesis of only goethite, SEM images were acicular, as expected; when only hematite was synthesized, the images of the samples were spherical. SEM images for the synthesis of goethite with distilled water plus Cys and artificial seawater plus Cys showed spherical crystal aggregates with radiating acicular crystals. For the other goethite synthesis experiments, we observed a mixture of acicular images (goethite) and spherical images (hematite).

For the synthesis of goethite in distilled water, distilled water plus Gly and artificial seawater plus Gly, the Mössbauer results (B_{hfs} values and areas) showed that only goethite was synthesized. For the synthesis of goethite with artificial seawater a doublet (20% of total area) due to isomorphic substitution of iron by seawater cations was observed. This result is in good agreement with that of EPR spectroscopy. The B_{hf} values for the samples of goethite synthesized with distilled water plus AIB and artificial seawater plus β-Ala were the same described for hematite. For these samples, a doublet arising from the interaction of iron with AIB or salts was observed. For iron hydroxide synthesis in distilled water plus Cys and artificial seawater plus Cys, Mössbauer results showed a B_{hf} consistent with the synthesis of goethite; doublet due to the interaction of iron with artificial seawater/Cys was also observed. It should be pointed out that EPR spectroscopy did not show this effect. For the other samples, B_{hf} values and areas indicated a mixture of goethite and hematite.

All results are showing that minerals are inherently complex; vary in composition due to dynamic synthesis conditions or the presence of organic substances, salts, metals, etc. Based on what was discussed above, a question must be answered: are these differences important for the interaction goethite/organic molecules? In our opinion this question could only be answered if experiments were performed using several different techniques (FT-IR, EPR, Mössbauer, X-ray, MEV, etc) for the analysis of the materials.

Acknowledgements

C. E. A. Carneiro and C. M. D. de Souza acknowledge the fellowship from Capes. This research was supported by grants from CNPq (no. 473076/2004) and Fundação Araucária (no. 2421). The authors are also grateful to Dr Célia G. T. de Jesus Andrade and Mr Osvaldo Capello from Laboratório de Microscopia e Microanálise for the MEV images.

References

Barrero, C.A., Betancur, J.D., Greneche, J.M., Goya, G.F. & Berquó, T.S. (2006). *Geophys. J. Int*. **164**, 331–339.

Berquó, T.S., Imbernon, R.A.L., Blot, A., Franco, D.R., Toledo, M.C.M. & Partiti, C.S.M. (2007). *Phys. Chem. Miner*. **34**, 287–294.

Biondi, E., Branciamore, S., Maurel, M.C. & Gallori, E. (2007). *BMC Evol. Biol*. **7**(Suppl 2), s2. doi:10.1186/1471-2148-7-S2-S2

Bishop, J.L. & Murad, E. (2002). *Geol. Soc. Lond. Spec. Publ*. **202**, 350–370.

Braterman, P.S., Cairns-Smith, A.G. & Sloper, R.W. (1983). *Nature* **303**, 163–164.

Carbone, C., Di Benedetto, F., Marescotti, P., Sangregorio, C., Sorace, L., Lima, N., Romanelli, M., Lucchetti, G. & Cipriani, C. (2005). *Mineral. Petrol*. **85**, 19–32.

Catling, D.C. & Moore, J.M. (2003). *Icarus* **165**, 277–300.

Cleaves, H.J. II, Scott, A.M., Hill, F.C., Leszczynski, J., Sahaide, N. & Hazen, R. (2012). *Chem. Soc. Rev*. **41**, 5502–5525.

Cohn, C.A., Hansson, T.K., Larsson, H.S., Soweby, S.J. & Holm, N.G. (2001). *Astrobiology* **1**, 477–480.

Cornell, R.M. & Schwertmann, U. (2003). *The Iron Oxides: Structure, Properties, Reactions, Occurrence and Uses*. Wiley-VCH Verlag GmbH & Co. KgaA, Weinheim, Federal Republic of Germany.

Cornell, R.M., Giovanoli, R. & Scheneider, W. (1990). *Clays Clay Miner*. **38**, 21–28.

Cudennec, Y. & Lecerf, A. (2006). *J. Solid State Chem*. **179**, 716–722.

Durmus, Z., Kavas, H., Toprak, M.S., Baykal, A., Altınçekiç, T.G., Aslan, A., Bozkurt, A. & Coşgun, S. (2009). *J. Alloys Compd*. **484**, 371–376.

Durmus, Z., Kavas, H., Baykala, A., Sozeri, H., Alpsoy, L., Çelik, M.S. & Toprak, S.Ü.C. (2011). *J. Alloys Compd*. **509**, 2555–2561.

Faivre, D. & Zuddas, P. (2006). *Earth Planet. Sci. Lett*. **243**, 53–60.

Fleming, G.D., Finnerty, J.J., Vallette, M.C., Celis, F., Aliaga, A.E., Fredes, C.F. & Koch, R. (2009). *J. Raman Spectrosc*. **40**, 632–638.

Flynn, C.M. Jr. (1984). *Chem. Rev*. **84**, 31–41.

Guskos, N. *et al*. (2002). *Mater. Res. Bull*. **37**, 1051–1061.

Holm, N.G. & Andersson, E. (2005). *Astrobiology* **5**, 444–460.

Holm, N.G., Dowler, M.J., Wadsten, T. & Arrhenius, G. (1983). *Geochim. Cosmochim. Acta* **47**, 1465–1470.

Holm, N.G., Ertem, G. & Ferris, J.P. (1993). *Orig. Life Evol. Biosph*. **23**, 195–215.

Holm, N.G., Dumont, M., Ivarsson, M. & Konn, C. (2006). *Geochem. Trans*. **7**, 7.

Kandori, K., Sakai, M., Inoue, S. & Ishikawa, T. (2006). *J. Colloid Interface Sci*. **293**, 108–115.

Kapitán, J., Baumruk, V., Kopecky, V. & Bour, P. (2006). *J. Phys. Chem. A* **110**, 4689–4696.

Kosmulski, M., Maczka, E., Jartych, E. & Rosenholmbet, J.B. (2003). *Adv. Colloid Interface Sci*. **103**, 57–76.

Lu, B., Li, P., Liu, H., Zhao, L.Y. & Wei, Y. (2011). *J. Phys. Chem. Solids* **72**, 1032–1036.

Mantion, A., Gozzo, F., Schmitt, B., Stern, W.B., Gerber, Y., Robin, A.Y., Fromm, K.M., Painsi, M. & Taubert, A. (2008). *J. Phys. Chem. C* **112**, 12104–12110.

Martin, W., Baross, J., Kelley, D. & Russell, M.J. (2008). *Nat. Rev. Microbiol*. **6**, 805–814.

Mohapatra, M., Rout, K. & Anand, S. (2009). *J. Hazard. Mater*. **171**, 417–423.

Moorbath, S. (1977). *Sci. Am*. **236**, 92–104.

Norén, K., Loring, J.S. & Persson, P. (2008). *J. Colloid Interface Sci*. **319**, 416–428.

Rietmeijer, F.J.M. (1996). *Meteorit. Planet. Sci*. **31**, 237–242.

Shanker, U., Bhushan, B., Bhattacharjee, G. & Kamaluddin (2012). *Orig. Life Evol. Biosph*. **42**, 31–45.

Smith, R.M., Motekaitis, R.J. & Martell, A.E. (1985). *Inorg. Chim. Acta* **103**, 73–82.

Uehara, G. (1979) *Mineral–Chemical Properties of Oxisols. International Soil Classification Workshop*, vol **2**, Soil Survey Division— Land Development Department, Bangkok, Thailand, p. 45–6.

Varanda, L.C., Morales, M.P., Jafelicci, M. & Serna, C.J. (2002). *J. Mater. Chem*. **12**, 3649–3653.

Vieira, A.P., Berndt, G., de Souza Junior, I.G., di Mauro, E., Paesano Junior, A., de Santana, H., da Costa, A.C.S., Zaia, C.T.B.V. & Zaia, D.A. M. (2011). *Amino Acids* **40**, 205–214.

Villalobos, M., Cheney, M.A. & Cienfuegos, J.A. (2009). *J. Colloid Interface Sci*. **336**, 412–422.

Wade, M.L., Agresti, D.G., Wdowiak, T.J. & Armendarez, L.P. (1999). *J. Geophys. Res*. **104**, 8489–8507.

Wang, G.H., Li, W.C., Jia, K.M., Spliethoff, B., Schüth, F. & Lu, A.H. (2009). *Appl. Catal. A* **364**, 42–47.

Wang, G.H., Li, W.C., Jia, K.M. & Lu, A.H. (2011). *Nano Brief Rep. Rev*. **6**, 469–479.

Webb, J., Macey, D.J., Chua-anusorn, W.T.G., Pierre, S.T., Brooker, L.R., Rahman, I. & Noller, B. (1999). *Coord. Chem. Rev*. **190–192**, 1199–1215.

Xiaojuan, Y., Huaimin, G. & Jiwei, W. (2010). *J. Mol. Struct*. **977**, 56–61.

Zaia, D.A.M. (2012). *Int. J. Astrobiol*. **11**, 229–234.

Zaia, D.A.M., Zaia, C.T.B.V. & de Santana, H. (2008). *Orig. Life Evol. Biosph*. **38**, 469–488.

Zhu, G., Zhu, X., Fan, Q. & Wan, X. (2011). *Spectrochim. Acta A* **78**, 1187–1195.

Zysler, R.D., Fiorani, D., Testa, A.M., Suber, L., Agostinelli, E. & Godinho, M. (2003). *Phys. Rev. B* **68**(1–4), 212408.